Environmental Science
Water Research & Technology

ROYAL SOCIETY OF CHEMISTRY

PAPER

View Article Online
View Journal | View Issue

Cite this: *Environ. Sci.: Water Res. Technol.*, 2021, **7**, 2231

Emerging investigator series: electrochemically-mediated remediation of GenX using redox-copolymers†

Paola Baldaguez Medina, Stephen Cotty, Kwiyong Kim, Johannes Elbert and Xiao Su *

Per- and polyfluorinated alkyl substances (PFAS) are persistent contaminants that have been continuously detected in groundwater and drinking water around the globe. Hexafluoropropylene oxide dimer acid (tradename GenX) has been used to substitute traditional PFAS, such as PFOA, but its intense use has caused widespread occurrence in water streams and often in high levels. Here, we evaluate a redox-copolymer, poly(4-methacryloyloxy-2,2,6,6-tetramethylpiperidin-1-oxyl-*co*-4-methacryloyloxy-2,2,6,6-tetramethylpiperidine) (PTMA-*co*-PTMPMA), for the selective electrochemical removal of GenX. The amine functional groups promote affinity towards the anionic PFAS, and the redox-active nitroxide radicals provide electrochemical control for adsorption and desorption. Faster kinetics and higher uptake (>475 mg g^{-1} adsorbent) were obtained with the redox-copolymer when applying 0.8 V *vs.* Ag/AgCl potential compared to open circuit. The copolymer electrosorbents were evaluated over a wide pH range and diverse water matrices, with electrostatic-based mechanisms dependent on the state of protonation of the PFAS. Moreover, we translated the redox-electrodes from a batch to flow-by cell configuration, showing successful adsorption and release of GenX under flow and electrochemical control. Finally, prolonged exposure of GenX at reduction potentials generated smaller PFAS fragments at the redox-electrodes. To fully defluorinate GenX, the copolymer-functionalized electrodes were coupled with a boron-doped diamond (BDD) counter electrode for integrating separation and defluorination within the same device. The combined system demonstrated close to 100% defluorination efficiency. Thus, we highlight the potential of electroactive redox platforms for the reactive separation of fluorotelomers, and point to future directions for their practical implementation for water treatment.

Received 31st July 2021,
Accepted 30th September 2021

DOI: 10.1039/d1ew00544h

rsc.li/es-water

Water impact

GenX is a new class of short-chain PFAS that led to increasing environmental concerns due to its ubiquitous occurrence. This study explores the capability of redox-copolymers consisting of TEMPO units to electrochemically capture and remove GenX from water streams. We demonstrate the high capacity of the redox electrodes for GenX adsorption in batch and flow-by cell systems. We also show the enhancement of kinetics with applied potential, and the ability to integrate the electrosorbents with boron-doped diamond (BDD) electrodes during regeneration for GenX defluorination.

1. Introduction

Poly and perfluoroalkyl substances (PFAS) are a large group of anthropogenic organic pollutants that have been extensively used since the 1950s.[1] Their chemical structure is composed of a strong carbon fluoride bond that increases their persistence in the environment, thus promoting the search for effective treatment technologies. Around six thousand PFAS are known, which have been classified by their hydrophilic moieties. The most abundant compounds are perfluoroalkyl acids which possess at least one negatively charged functional group, commonly carboxylic or sulfonic acids. PFAS contain oleophobic and hydrophobic characteristics that are attractive for a range of commercially available products such as firefighting foams, non-stick cookware, food packaging, cosmetics, and many more.[2–5] Consequently, these ubiquitous compounds have been found in soil, landfills, air, and water, and their potential toxicity and bioaccumulation have caused global concern.[6–9] Contaminated water is suspected to be the primary route of exposure to humans.[10]

Chemical and Biomolecular Engineering, University of Illinois at Urbana-Champaign, Urbana, Illinois, 61801, USA. E-mail: x2su@illinois.edu

† Electronic supplementary information (ESI) available. See DOI: 10.1039/d1ew00544h

Therefore, the U.S. Environmental Protection Agency (EPA) and the European Commission declared advisory levels for drinking water of 70 ng L^{-1} and 0.5 μg L^{-1}, respectively, to reduce the spread of these compounds into consumable water.[11,12] PFAS have been detected in aquatic and drinking water at levels that greatly surpass the EPA and European Commission standards.[8,13–16] For example, Veneto, Italy, has been one of the places where the abundant concentration of PFAS has been found in drinking water,[14] with concentration levels ranging from 319 to as high as 1475 ng L^{-1}.[14] In the United States, surface water has been found to contain levels of PFAS up to 2000 ng L^{-1}, and in surface water foams, up to 97 000 ng L^{-1}.[17,18] Also, in some instances of groundwater, PFAS concentrations have been found at levels as high as 5200 ng L^{-1}.[19] Associated with this widespread occurrence, numerous studies have shown their presence in human blood serum and wildlife, which is indicative of the importance of monitoring and implementation of targeted treatment methods.[20–22]

Most studies of PFAS adsorption and destruction have focused on perfluorooctanoic acid (PFOA) and perfluorooctanesulfonic acid (PFOS). These two compounds were found more broadly and at much higher concentrations than other PFAS in water,[23] being amongst the original PFAS developed in the early 1940s.[1] However, with increasing stringent regulations for PFOA and PFOS,[11] there has been a rise in the use of short chain PFAS as alternatives. Among these, hexafluoropropylene oxide dimer acid (HFPO-DA, also known as GenX) has seen rapidly increasing use as a direct substitute of PFOA,[24] and being utilized in even larger quantities than PFOA, to match the performance of longer chain precursors.[25] While GenX could potentially have lower bioaccumulation properties based on their volatility and C–F distribution, it has increasingly been detected in water, with these short-chain compounds as well as their degradation by-products persisting in the environment.[26]

The molecular properties of GenX present several challenges for separation processes and environmental remediation. The shorter aliphatic backbone of GenX, along with the middle ether bond, makes it more hydrophilic when compared with longer chain PFAS. Also, these shorter chain PFAS present higher mobility in the environment, increasing their chances of being found in water streams and even drinking water.[27,28] GenX also exhibits high water solubility due to its pK_a of 2.84, which provides the molecule with a negative charge over a wide pH range.[29] Previous studies have targeted GenX for water remediation using conventional treatment techniques such as adsorption, ion exchange, filtration, and reverse osmosis.[30,31] For adsorption based techniques, short-chain PFAS still suffer from regeneration efficiency limitations,[30,32] and limited molecular selectivity. In addition, traditional chemical adsorption methods require the input of additional chemicals and solvents for regeneration, which increases the operating cost of the process as well as chemical footprint.[33]

Thus, an electrochemical route for separation and remediation of PFAS can provide an attractive platform that is environmentally friendly, by reducing energy and chemical costs. Recently, electrochemical pathways have been explored for the efficient removal and remediation of emerging contaminants in water by leveraging molecularly-tailored interfaces for selective electrosorption and destruction.[34–38] In particular, our previous study has leveraged redox-copolymers for the selective binding and integrated defluorination of long-chain PFAS.[36] It revealed that three main interactions – hydrophobicity, amine interactions, and electrostatic interactions – could be tuned to synergistically capture/release traditional PFAS such as PFOA and PFOS without the use of a chemical regenerant.

However, redox electrosorbents have not yet been evaluated for shorter chain PFAS such as GenX – which is a critical gap for the performance of these redox systems due to the increased occurrence of these new classes of PFAS. Here, we selected a copolymer that combines 4-methacryloyloxy-2,2,6,6-tetramethylpiperidin-1-oxyl (TMA) and 4-methacryloyloxy-2,2,6,6-tetramethylpiperidine (TMPMA) repeating units, explicitly PTMA-*co*-PTMPMA (Fig. 1), proven to be effective in adsorbing long-chain PFAS in our previous study.[36] Amine functionalities have been regarded as a superior binding site with affinity for negatively charged PFAS,[39,40] and the secondary amine functionality (N–H) of the piperidine unit exhibits a high pK_a value (pK_a = 11.28),[41] providing protonated and thus positively charged binding sites toward negatively charged GenX in a wide range of pH values. At the same time, the redox couple of a nitroxide radical/oxoammonium (N–O·/N=O$^+$) allows for additional enhancement in the electrostatic interactions with the anionic carboxylate group of GenX and serves as a reversible, electrochemically-mediated switch for adsorption and regeneration.

In this work, we investigated redox-electrodes functionalized with PTMA-*co*-PTMPMA as an electrosorbent for short-chain PFAS, specifically GenX. The redox-electrode system was proven to adsorb GenX selectively when an oxidative potential is applied, and the ability to release bound GenX at a reductive potential (Fig. 2). We investigated the balance of electrostatic *vs.* hydrophobic interaction at different pH values, and the application of our electrosorbent to a range of environmentally relevant water matrices. Also,

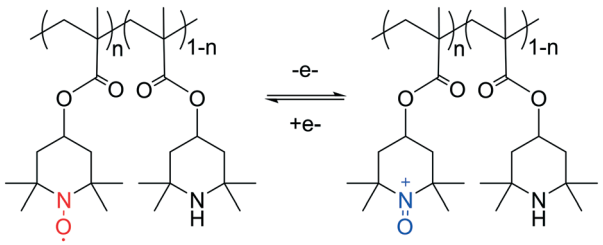

Fig. 1 Redox-active PTMA-*co*-PTMPMA copolymer utilized to increase the adsorption uptake *via* electrochemical input. The nitroxide radical group when oxidized becomes an oxoammonium cation, controlling the electrostatic interactions, while the N–H secondary amine counterpart (PTMPMA) enhances adsorption based on affinity to the amine groups.

the redox electrodes were translated from a batch analytical scale to a larger flow cell system, to showcase the ability of the redox-electrodes for adsorbing/desorbing GenX through electrochemical modulation for more relevant practical processes. Finally, we examined the reductive degradation of GenX using a combined asymmetric redox-copolymer//boron-doped diamond (BDD) configuration, where the BDD counter electrode was shown to be effective for the defluorination of the released GenX.

2. Materials and methods

2.1 Materials

Undecafluoro-2-methyl-3-oxahexanoic acid (GenX) (97%) was obtained from Matrix Scientific. All other chemicals were obtained from Sigma Aldrich, VWR, Fisher Scientific, or TCI, and they were used as received. Acetonitrile and ammonium acetate for LC/MS analysis were of LC grade. Water for LC/MS and ion chromatography (I.C.) analysis was obtained from an ELGA Purelab Flex 1 system >18 MΩ. The stock solution for each PFAS compound was prepared in DI water at a concentration of 10 mM without supporting electrolytes, which was diluted to prepare a range of starting solutions for electrochemical tests. These solutions were stored in the fridge (4 °C), and the storage time was no longer than six months.

2.2 Analytical methods for PFAS and fluoride detection

A Waters Synapt G2Si with Waters Acquity H-class UPLC LC/MS system was used to detect the PFAS concentration in an aqueous solution. All parameters utilized for the LC/MS analysis can be found in the ESI† of this work (Section S1.5). For detecting the fluoride content, a Thermo Fisher Dionex 2100 ion chromatography system (I.C.) was utilized. The analytical parameters used have been described elsewhere.[36] For each analytical run, a new set of calibration curves were assessed for both LC/MS and (I.C.).

2.3 Electrode preparation and characterization

The polymer-coated electrodes of PTMA-*co*-PTMPMA/multi-walled carbon nanotubes (MWCNTs) were prepared using a dip-coating technique, which is described in detail in the ESI† (Section S1.2). PTMA-*co*-PTMPMA has been previously synthesized, with a product composed of 51 mol% TMA and 49 mol% TMPMA.[36] This copolymer is known for its optimal triple interactions with long-chain PFAS and dispersion with multi-walled carbon nanotubes that serve as an excellent binder to improve the surface area and conductivity. The ink solution ratio was composed of 1 : 1 PTMA-*co*-PTMPMA : MWCNT and was applied onto the stainless-steel mesh electrode *via* a dip-coating technique and dried with air. The loading mass was maintained at 0.5 mg in an active surface area of 2 cm^2.

2.4 Electrochemical experiments

Electrochemical experiments were carried out in a potentiostat (SP-200 Potentiostat, Biologic, and Squidstat Plus, Admiral Instruments). For batch electrosorption and release experiments, a BASi VC-S voltammetry electrochemical cell in a three-electrode configuration was used. Ag/AgCl was used as the reference electrode, and Pt was used as the counter electrode for all adsorption experiments. Batch experiments were performed in 5 mL solutions unless otherwise specified. The typical electrosorption time was 30 min, with a solution containing 20 mM NaCl, unless otherwise indicated. All the adsorption calculations were performed using the total mass of the polymer and multi-walled carbon nanotubes added together. Error bars are shown for standard errors of the mean on replicate experiments. Based on the results obtained in Fig. S12,† the MWCNT itself was shown to have some limited adsorption towards GenX.

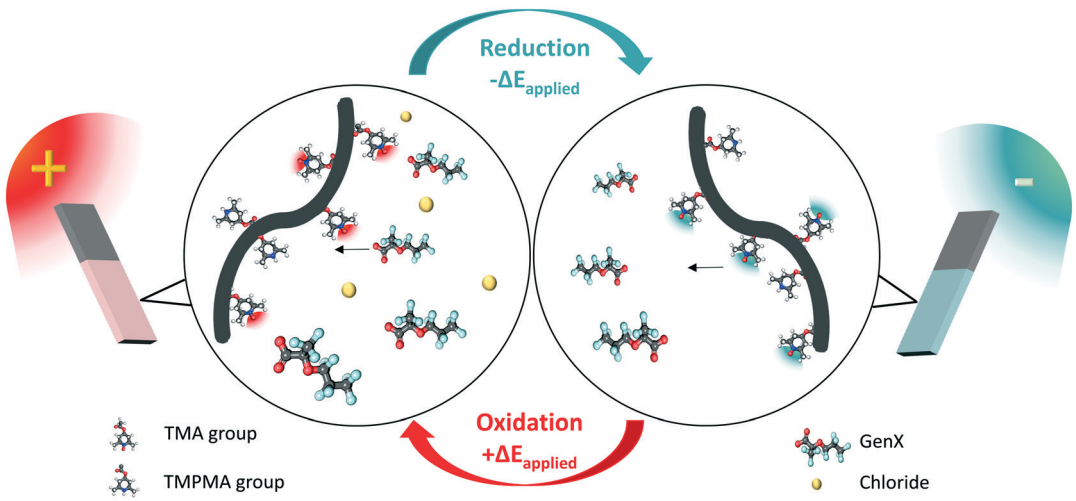

Fig. 2 A representative scheme of the redox-active electrode of PTMA-*co*-TMPMA for the electrochemical adsorption and desorption of GenX in the presence of competing anions. An oxidative potential promotes the selective electrosorption of the anionic PFAS, while a reductive potential releases the bound molecules.

2.5 Electrochemical flow cell

For flow cell experimentation, a custom in-house flow-by cell was utilized in a two-electrode configuration, with 16 cm^2 area (4 cm × 4 cm) electrodes. The working electrodes were coated with the PTMA-*co*-PTMPMA/MWCNT solution using a drop-casting technique. Either a bare titanium or a platinum (Pt) sputter-coated (Pt thickness of 251.0 nm) titanium plate was used as a counter electrode. All the experiments were performed using chronopotentiometry by applying 2 mA for adsorption and −2 mA for desorption with a GenX flow rate of 1 mL min^{-1} from a Longer Instruments peristaltic pump.

3. Results and discussion

3.1 PTMA-*co*-PTMPMA electrode fabrication and characterization

PTMA-*co*-PTMPMA was synthesized by oxidation of PTMPMA with meta-chloroperoxybenzoic acid (MCPBA), as described previously.[36] The content of nitroxide radicals was found to be 51 mol%, determined by ultraviolet-visible spectroscopy at 460 nm absorption wavelength.[36] The presence of nitroxide and amine functionalities on the electrode was confirmed by X-ray photoelectron spectroscopy (XPS) (Fig. S4†). The lower binding energy peak (400 eV) corresponds to the N–H functional group, while the N–O· peak can be found at 402 eV. The cyclic voltammogram in Fig. 3a indicated that oxidation of the N–O· to N═O^+ occurred at 0.83 V *vs.* Ag/AgCl, while reduction occurred at 0.53 V *vs.* Ag/AgCl. In addition, contact angle measurements show the hydrophobic properties of PTMA-*co*-PTMPMA, which can be expected to be beneficial for GenX uptake (Fig. S5†).

3.2 Electrosorption of GenX

Before each electrochemical measurement, we carried out a pre-treatment step to ensure all electrodes possessed the same state of charge (fully discharged, with no counter ion bound). For pre-treatment, cyclic voltammetry was carried out from 0.0 to 1.2 V *vs.* Ag/AgCl in 0.1 M $NaClO_4$ solution (Fig. 3a). Then, the electrode was reduced in the same solution by chronoamperometry with 0.0 V *vs.* Ag/AgCl for 3 minutes. Without pre-activation, redox-electrodes showed lower uptake capacities, as observed in Fig. S1.† Based on these results (Fig. S1†), we hypothesized that by fully reducing the electrode, the adsorption sites that promote higher hydrophobic interactions and electrostatic attractions can be activated simultaneously when applying an anodic potential and consequently increase the kinetics for the adsorption reaction. Electrochemical separation of GenX at different potentials was carried out in 0.1 mM + 20 mM NaCl solution. We used 0.1 mM GenX as a way to understand the competitive behaviour of the target PFAS ions towards various electrode chemistries and potentials at higher

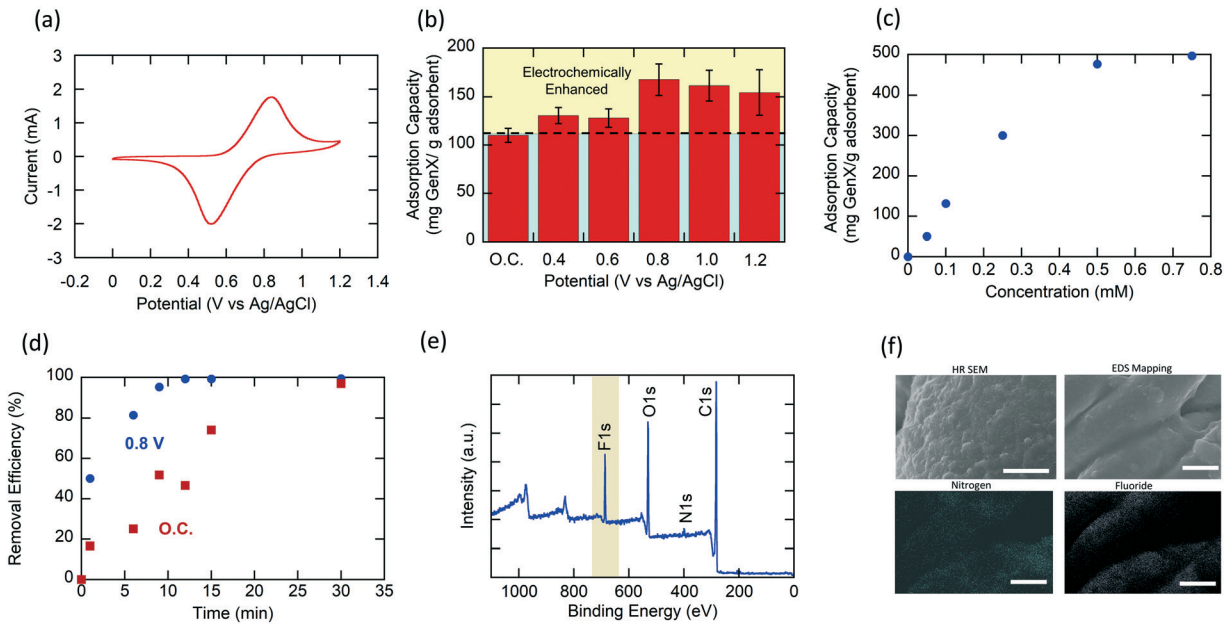

Fig. 3 Characterization of PTMA-*co*-PTMPMA. (a) Cyclic voltammogram of PTMA-*co*-PTMPMA in 0.1 M $NaClO_4$. Scan rate of 10 mV s^{-1} in a range from 0.0 to 1.2 V *vs.* Ag/AgCl. (b) Electrochemical uptake of PTMA-*co*-PTMPMA at different potentials. The experiments were performed in 0.1 mM GenX and 20 mM NaCl for 30 minutes applying continuous stirring of 300 rpm. Error bars correspond to three consecutive experiments. (c) GenX equilibrium isotherm for PTMA-*co*-PTMPMA with 0.8 V *vs.* Ag/AgCl for different GenX concentrations in 20 mM NaCl. (d) Comparison of adsorption kinetics of PTMA-*co*-PTMPMA at open circuit compared to 0.8 V *vs.* Ag/AgCl. The experiment was performed with 0.1 mM GenX and 20 mM NaCl. (e) XPS survey of an electrode after being adsorbed in 0.1 mM GenX and 20 mM NaCl. Fluoride peak of F1s shows high intensity proving the adsorption of the PFAS compound. (f) Scanning electron microscopy (SEM) figures of a PTMA-*co*-PTMPMA electrode after 12 hours of electrosorption at 0.8 V *vs.* Ag/AgCl. Energy-dispersive X-ray spectroscopy (EDS) mapping highlights fluoride adsorption. The scale bar for the high-resolution image is 5 μm, SEM and EDS mapping on N/F are 20 μm.

concentrations. Later, lower concentrations in the ppb range are used for simulated water matrices. The highest uptake capacity for the redox-copolymer functionalized electrodes was observed at 0.8 V *vs.* Ag/AgCl (Fig. 3b). At potentials higher than 0.83 V *vs.* Ag/AgCl, *e.g.* above the oxidation peak of PTMA-*co*-PTMPMA (Fig. 3a), the uptake capacity decreased possibly due to competing adsorption of chloride caused by enhanced capacitive effects.

Based on an energy consumption calculation at different potentials (Fig. S13a†), 0.8 V *vs.* Ag/AgCl was selected as an optimal operating condition due to lower energetic costs. When comparing adsorption at an electric potential at 0.8 V with open circuit adsorption, it was found that applying charge to the system enhanced the adsorption uptake capacity by more than 50 mg g^{-1} (Fig. 3b). These findings prove the importance of additional electrostatic attractions of the oxoammonium cations in oxidized PTMA-*co*-PTMPMA towards the short-chain GenX PFAS. An equilibrium isotherm study revealed that at different concentrations, our system exhibited an uptake capacity of up to 497 mg g^{-1} adsorbent when applying 0.8 V *vs.* Ag/AgCl for 30 minutes (Fig. 3c). The isotherm result was fitted using the Langmuir and Freundlich models. The Langmuir model portrays a better fit based on the correlation coefficient (R^2 = 0.997 for Langmuir, *vs.* R^2 = 0.934 for Freundlich) (Fig. S7 and Table S3†).

Time-dependent measurements were carried out to study the adsorption kinetics, at both open circuit (O.C.) and 0.8 V *vs.* Ag/AgCl, using 2.5 mL of 0.1 mM GenX and 20 mM NaCl (Fig. 3d). Interestingly, electrostatic enhancement promoted >95% of GenX removal in just 9 minutes, while for O.C., the reaction reached >95% removal only after 30 minutes. Linear fitting using the pseudo-first-order and pseudo-second-order kinetics model were used to estimate kinetic parameters. The best-fitting model for 0.8 V *vs.* Ag/AgCl was a pseudo-second-order kinetics model, with a rate constant of 0.00894 g mg^{-1} min^{-1} (Fig. S8 and Table S4†). In contrast, kinetics results for open circuit experiments showed a better fit with the pseudo-first-order kinetic model, based on the correlation coefficient. The rate constant for the open circuit experiment (based on the pseudo-first-order models) was 0.00268 min^{-1} (Fig. S9 and Table S5†). Our results showed comparable kinetics to other state-of-art materials such as ion exchange resins.[32]

XPS analysis performed on an adsorbed PTMA-*co*-PTMPMA/MWCNT electrode after applying a 0.8 V potential in 0.1 mM GenX and 20 mM NaCl indicated a ratio of 9.85 between F^- and Cl^-, which was equal to a 0.89 GenX/Cl^- ratio, accounting for the number of fluorines in a Gen-X molecule (11). The separation factor was calculated using eqn (1), with the results showing a separation factor of 178 for GenX, indicating the high selectivity of our redox polymer toward GenX over competing chloride.

$$\text{Separation Factor}_{\text{GenX}^-/\text{Cl}^-} = \frac{\frac{q_{F^-}}{q_{Cl^-}}}{11 \times C_{\text{GenX}^-_0}/C_{\text{Cl}^-_0}} \quad (1)$$

$C_{\text{GenX}^-_{eq}}$ and $C_{\text{Cl}^-_{eq}}$ are the initial concentrations of their respective species in solution, 0.1 mM for GenX and 20 mM for NaCl, while the ratio of the solid phase uptake of q_{F^-} and q_{Cl^-} was estimated from the XPS analysis, 90.78% for F^- and 9.22% for Cl^-. Fig. 3e further confirms the successful electrosorption of GenX based on the intense fluoride peak found after adsorption. Also, Fig. 3f shows a high-resolution scanning electron microscopy (SEM) image of the surface of a new electrode as well as an EDS mapping of PTMA-*co*-PTMPMA/MWCNT electrode ran for 30 min at 0.8 V *vs.* Ag/AgCl in 0.1 mM GenX and 20 mM NaCl, where fluoride could be detected after 30 minutes of electrosorption.

3.3 Electroseparation in various water matrices and pH effect

We studied the effect of solution pH on the adsorption of GenX with PTMA-*co*-PTMPMA. GenX's pK_a is 2.84, indicating that it would exist in the anionic form at a higher pH level.[29] At pH 1.9, GenX is mostly found in its neutral/protonated form, and hydrophobic interaction is hypothesized to be the dominant interaction for adsorption – note that there was no electrochemically-driven enhancement observed (Fig. 4a). At pH > 4, the adsorption would be mainly ascribed to electrostatic interactions since now GenX exists in the anionic form. Therefore, in the pH range of 4 to 9, applying a positive potential exhibited better adsorption compared to open circuit. At the higher pH region >9, competition between GenX and hydroxide counter ions seems to hinder the adsorption of GenX. Also, considering that the pK_a of the piperidine group is 11.28,[41] the polymer becomes deprotonated at a very high pH, and therefore, the hydrophobic interaction becomes the dominant binding interaction. We observe that GenX adsorption was decreased when applying 0.8 V *vs.* Ag/AgCl at pH 13.5, Fig. 4a.

The impact of the sodium chloride concentration was studied for 0.1 mM GenX (Fig. 4b). Our findings show almost no change in adsorption capacities from 5 to 100 mM NaCl, while the adsorption under highly saline conditions[42] (500 mM NaCl) was poor. The high concentration of competing ions screens the positive charges on the polymer, thus weakening electrostatic interactions with the GenX species. In addition, different water matrices and low concentrations of GenX were studied to test our system under near environmental conditions (Fig. 4c). The water matrices studied were tap water and municipal secondary wastewater effluent (SWE, from the Urbana-Champaign Sanitary District). The water specifications of the secondary wastewater effluent can be found in ESI† Section S1.6. The selected concentrations were 100 ppb and 15 ppb of GenX in 20 mM NaCl based on the high levels of PFAS that had been found in surface and groundwater.[17,18,43] Tap water and SWE were spiked with 0.1 mM of GenX, and both achieved >40% removal efficiency after 3 hours of electrosorption. Meanwhile, ultra-diluted samples showed >55% removal efficiency under the same experimental conditions.

We also translated the batch scale system into an electrochemical flow-by cell device containing a 16 cm^2 (4 cm

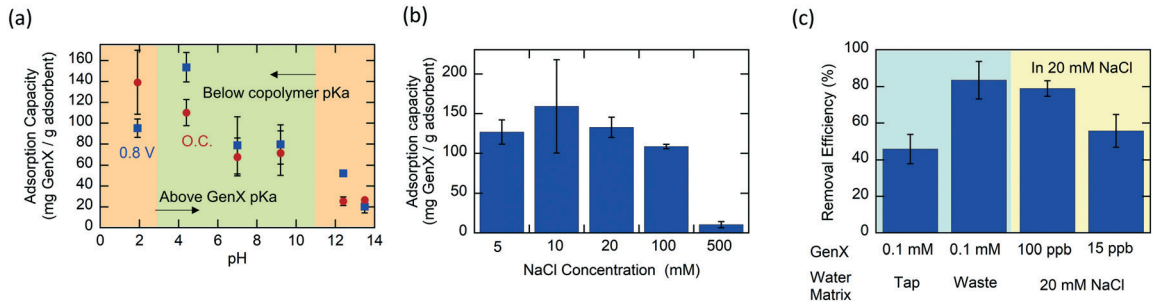

Fig. 4 (a) Adsorption capacity of PTMA-*co*-PTMPMA towards GenX at different pH values. Experiments were performed in 0.1 mM GenX and 20 mM NaCl with 0.8 V for 30 minutes. (b) Adsorption capacity of PTMA-*co*-PTMPMA at varying ionic strength and 0.1 mM GenX at 0.8 V *vs.* Ag/AgCl. (c) Removal efficiency using different water matrices and lower concentrations of GenX in 20 mM NaCl for 3 hours. All error bars correspond to two experiments.

× 4 cm) working electrode with 8 mg of PTMA-*co*-PTMPMA coating, and an equal dimension titanium counter electrode for the adsorption and release of GenX. Fig. 5 shows the schematics of our flow cell system, and the assembly method is described in the ESI† (Section S1.3). Prior to electrochemical GenX adsorption, a 0.1 mM GenX solution was cycled through the flow cell apparatus (1 mL min^{-1}) at open circuit for 24 hours to allow the system to equilibrate. Electrochemical GenX adsorption was then carried out *via* application of a constant +2 mA current for 30 minutes, at which 109 mg g^{-1} adsorbent was achieved with an energy consumption of 1 kJ g^{-1} adsorbent (2 kJ g^{-1} copolymer). The linear uptake profile in Fig. 5 indicates that complete saturation of the electrode did not occur within 30 minutes and the adsorption equilibrium of GenX is likely to be higher given more time. Following adsorption, the flow cell inlet was changed to a pristine solution containing no GenX and allowed to flush for 10 minutes at open circuit. During the solution change-over, very little GenX was observed to release into the pristine solution, and the uptake was equilibrated to 100 mg g^{-1}, indicating little to no concentration equilibrium-based release mechanism.

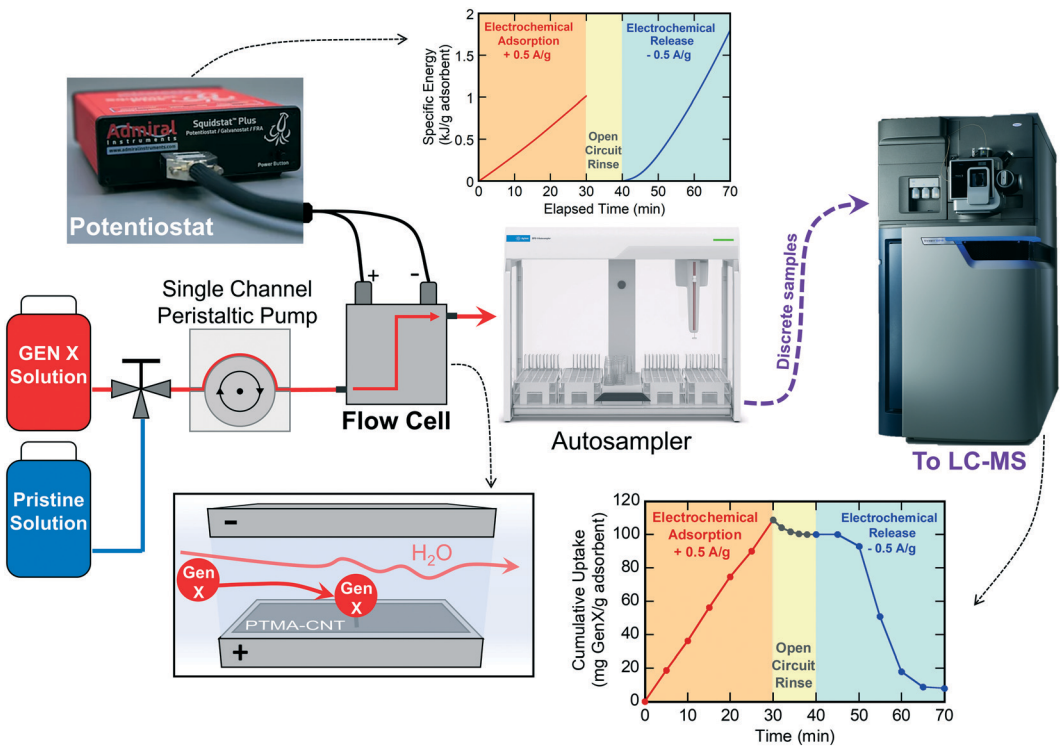

Fig. 5 Electrochemical flow cell schematic. A 0.1 mM GenX solution and a 20 mM NaCl solution enter the peristaltic pump towards the flow cell. The GenX solution could be switched to a 20 mM NaCl solution (pristine solution) for desorption. The chronopotentiometric experiments were controlled with a potentiostat and the resulting samples were collected and analysed with LC–MS. The figure also illustrates a flow cell experiment of GenX after pre-treating and pre-equilibrating the PTMA-*co*-PTMPMA electrode, indicating the cumulative uptake of GenX. The counter electrode used in this experiment was Ti.

After adsorption, a constant current of −2 mA was applied, releasing bound GenX into a pristine flowing solution. The system showed a regeneration efficiency of 93% after 30 minutes, with 1.80 kJ g^{-1} adsorbent (3.5 kJ g^{-1} copolymer) energy consumed. The flow cell results showcase the potential of the PTMA-*co*-PTMPMA electrochemical adsorption platform for continuous adsorption applications in GenX remediation, and highlight the importance of potential in the GenX removal process, where the bound GenX was only released once a reducing current was applied.

3.4 Electrode regeneration and an asymmetric release-destruction system

Once a negative potential is applied, the N═O$^+$ sites were reduced to its original radical (N–O·) state, promoting the release of the GenX molecule by electrostatic repulsion. Different release/regeneration potentials were tested, ranging from −1.5 V to 0.0 V *vs.* Ag/AgCl for 1 hour (Fig. S11†). The results indicated that decreasing potentials led to higher release of GenX. We selected −1 V *vs.* Ag/AgCl for our tests as a representative potential, with a comparison between GenX release at −1 V *vs.* Ag/AgCl and open circuit shown in Fig. 6a. Applying a reductive potential was shown to enhance desorption compared to open circuit, with a release of GenX > 80%, after one hour of electrochemical operation (Fig. 6a).

Next, cyclability tests of our system were performed for 5 cycles of electrosorption and electrochemical release. During electrosorption, a potential of 0.8 V *vs.* Ag/AgCl was applied for 30 min, with a solution of 5 mL of 0.1 mM GenX and 20 mM NaCl for adsorption. For desorption, a −1.0 V *vs.* Ag/AgCl potential was applied, and the system was reduced for 1 hour into 20 mM NaCl. This process was repeated for five full cycles, and the results shown in Fig. S16† indicate that the adsorption capacity of our system was maintained. Interestingly, the regeneration efficiency of our system (the amount of GenX recovered during release relative to that adsorbed) decreased considerably, and after four cycles, it was maintained for up to 20% regeneration efficiency (*e.g.*, GenX released).

As such, we hypothesized that partial degradation of GenX could have occurred during reductive regeneration (Fig. S20†). High-resolution mass spectroscopy analysis was performed on a solution that mimics a typical release concentration after an adsorption cycle. This concentration was 0.024 mM GenX + 20 mM NaCl, and the mass spectra were analysed after applying −1.0 V *vs.* Ag/AgCl (Fig. S23†) for one hour to evaluate whether there was any electrochemically-mediated degradation (see the chromatogram comparison in Fig. S22 and HR-MS spectra in Fig. S23 and S24†). The HR-MS peak analysis seemed to indicate that GenX degradation could potentially occur at the carboxylate group and through breakage of the ether bond. Our results support our hypothesis that GenX could be degraded at reductive potentials and longer treatment times for regeneration, leading to seemingly low regeneration efficiency for separation, yet preserved the adsorption capacity. A more detailed analysis will be carried out in future studies to develop a full mechanistic model for GenX breakdown at redox-electrodes, and under varying electrochemical conditions.

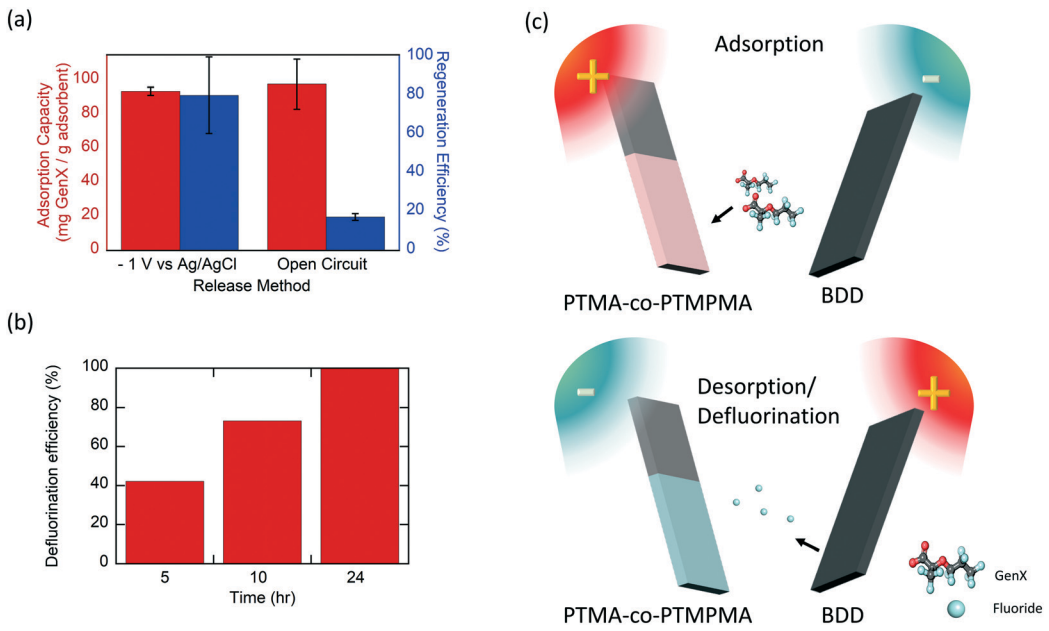

Fig. 6 (a) A comparison of the regeneration efficiency of the redox-electrodes between −1 V *vs.* Ag/AgCl and open circuit (OC) for GenX release. Adsorption was performed for 30 minutes at 0.8 V *vs.* Ag/AgCl, in 0.1 mM GenX and 20 mM NaCl. (b) Defluorination of BDD as a function of time, at 10 mA cm^{-2}. The defluorination was carried out in 20 mM NaCl solution, after GenX was released from a loaded electrode. (c) Scheme illustrating the synergistic adsorption/defluorination with PTMA-*co*-PTMPMA as an electrosorbent and BDD as a reactive working electrode.

The consequences from the formation of these new by-products have not been fully studied, but based on their similar chemical structures as their former PFAS versions, these C–F by-products could still be recalcitrant.[44] As such, full defluorination to fluoride should be ideally achieved as a pathway for complete remediation of these short-chain PFAS. Therefore, we decided to incorporate boron doped diamond (BDD) electrodes into the electrochemical system to increase the defluorination efficiency and further break down into fluoride during the release step. We combined our system with BDD counter electrodes, into an integrated PTMA-*co*-PTMPMA//BDD configuration for the purpose of reactive separation and defluorination of GenX within a single device. BDD served as an efficient candidate for defluorination since it can generate hydroxyl radicals at high overpotentials that are able to cleave the C–F bond of the PFAS,[45–47] while displaying significant chemical and electrochemical stability.[48] Therefore, we evaluated an integrated electrochemical system for first electrosorbing GenX and later simultaneously defluorinating the PFAS during the release step at the counter electrode, as shown in Fig. 6c. We first adsorbed on PTMA-*co*-PTMPMA for 30 minutes by applying 0.8 V *vs.* Ag/AgCl, and then reversed the polarity and desorbed from the PTMA-*co*-PTMPMA electrode, simultaneously defluorinating with the help of BDD, by applying 10 mA cm^{-2} under continuous stirring (500 rpm). Our results indicate gradual defluorination behaviour with time (Fig. 6b), and after 24 h operation at 10 mA cm^{-2}, our system was able to release adsorbed GenX completely, and achieve 100% defluorination efficiency.

Conclusions

Here, we demonstrated the effectiveness of an electrochemically-mediated system for the electrosorption of GenX, using a PTMA-*co*-PTMPMA redox-copolymer containing nitroxide and amine moieties. The electrochemical removal performance of the redox-copolymers was evaluated across a range of GenX concentrations, in different water matrices, pH values, and ionic strengths, proving the effectiveness of these tailored functional electrodes for the adsorption of GenX. In particular, our work highlights the enhancement of adsorption kinetics under electrochemical conditions, which showed >95% of GenX removal in 9 minutes *versus* 30 minutes for >95% removal at O.C. At different pH values, the adsorption mechanism could be ascribed to varying degrees of hydrophobic affinity or electrostatic attraction, depending on the protonation characteristics of both the electrode and the PFAS. The redox-electrodes were shown to release GenX and re-adsorb for sequential cycles without significant drops in uptake capacity. We also demonstrated the potential integration of the redox-electrodes with defluorination systems such as BDD for tandem removal and remediation of GenX for up to 100% defluorination after 24 hours. Finally, the redox-electrodes were translated to a flow cell system, confirming that the electrosorption and release of GenX could be modulated under continuous electrosorption conditions. We envision future studies to improve on electrochemical reactor engineering, such as optimization of the electrode architecture and flow-cell configuration to maximize mass transfer and enhance the electrosorption kinetics. Further mechanistic studies are also needed for studying the full pathways for short-chain degradation with different redox-electrode materials.

Conflicts of interest

There are no conflicts to declare.

Acknowledgements

This work was supported by the University of Illinois, Urbana-Champaign (UIUC), the National Science Foundation under Grant #1931941, and the Illinois Innovation Network (IIN) seed grant. SEM and XPS analysis were carried out in the Frederick Seitz Materials Research Laboratory Central Research Facilities, University of Illinois. LC–MS was carried out in the School of Chemical Science (SCS) Mass Spectrometry Lab. The authors thank Angelique Klimek for assistance in electrode fabrication, Riccardo Candeago for assistance in preparing coated electrodes for flow cell experimentation, and Prof. Roland Cusick (CEE, UIUC) for the access to the UIUC CEE shared facilities. The authors would like to thank the NSF GRFP for fellowship funding to P. B. M, and the National Research Foundation of Korea (NRF) Ministry of Education for fellowship funding to K. K. (2020R1A6A3A03039138).

Notes and references

1 A. B. Lindstrom, M. J. Strynar and E. L. Libelo, Polyfluorinated Compounds: Past, Present, and Future, *Environ. Sci. Technol.*, 2011, **45**, 7954–7961.
2 Z. Wang, J. M. Boucher, M. Scheringer, I. T. Cousins and K. Hungerbühler, Toward a Comprehensive Global Emission Inventory of C4–C10 Perfluoroalkanesulfonic Acids (PFSAs) and Related Precursors: Focus on the Life Cycle of C8-Based Products and Ongoing Industrial Transition, *Environ. Sci. Technol.*, 2017, **51**, 4482–4493.
3 H. D. Whitehead, M. Venier, Y. Wu, E. Eastman, S. Urbanik, M. L. Diamond, A. Shalin, H. Schwartz-Narbonne, T. A. Bruton, A. Blum, Z. Wang, M. Green, M. Tighe, J. T. Wilkinson, S. McGuinness and G. F. Peaslee, Fluorinated Compounds in North American Cosmetics, *Environ. Sci. Technol. Lett.*, 2021, **8**, 538–544.
4 A. G. Paul, K. C. Jones and A. J. Sweetman, A First Global Production, Emission, And Environmental Inventory For Perfluorooctane Sulfonate, *Environ. Sci. Technol.*, 2009, **43**, 386–392.
5 A. Timshina, J. J. Aristizabal-Henao, B. F. Da Silva and J. A. Bowden, The last straw: Characterization of per- and polyfluoroalkyl substances in commercially-available plant-based drinking straws, *Chemosphere*, 2021, **277**, 130238.

6 J. M. Conder, R. A. Hoke, W. D. Wolf, M. H. Russell and R. C. Buck, Are PFCAs Bioaccumulative? A Critical Review and Comparison with Regulatory Criteria and Persistent Lipophilic Compounds, *Environ. Sci. Technol.*, 2008, **42**, 995–1003.

7 M. L. Brusseau, R. H. Anderson and B. Guo, PFAS concentrations in soils: Background levels versus contaminated sites, *Sci. Total Environ.*, 2020, **740**, 140017.

8 X. C. Hu, D. Q. Andrews, A. B. Lindstrom, T. A. Bruton, L. A. Schaider, P. Grandjean, R. Lohmann, C. C. Carignan, A. Blum, S. A. Balan, C. P. Higgins and E. M. Sunderland, Detection of Poly- and Perfluoroalkyl Substances (PFASs) in U.S. Drinking Water Linked to Industrial Sites, Military Fire Training Areas, and Wastewater Treatment Plants, *Environ. Sci. Technol. Lett.*, 2016, **3**, 344–350.

9 M. E. Morales-McDevitt, J. Becanova, A. Blum, T. A. Bruton, S. Vojta, M. Woodward and R. Lohmann, The Air That We Breathe: Neutral and Volatile PFAS in Indoor Air, *Environ. Sci. Technol. Lett.*, 2021, **8**, 897–902.

10 A. O. De Silva, J. M. Armitage, T. A. Bruton, C. Dassuncao, W. Heiger-Bernays, X. C. Hu, A. Kärrman, B. Kelly, C. Ng, A. Robuck, M. Sun, T. F. Webster and E. M. Sunderland, PFAS Exposure Pathways for Humans and Wildlife: A Synthesis of Current Knowledge and Key Gaps in Understanding, *Environ. Toxicol. Chem.*, 2021, **40**, 631–657.

11 Lifetime Health Advisories and Health Effects Support Documents for Perfluorooctanoic Acid and Perfluorooctane Sulfonate, https://www.epa.gov/ground-water-and-drinking-water/supporting-documents-drinking-water-health-advisories-pfoa-and-pfos, (accessed 2021).

12 Chemicals Strategy for Sustainability Towards a Toxic-Free Environment, https://ec.europa.eu/environment/pdf/chemicals/2020/10/SWD_PFAS.pdf, (accessed 2021).

13 R. H. Anderson, G. C. Long, R. C. Porter and J. K. Anderson, Occurrence of select perfluoroalkyl substances at U.S. Air Force aqueous film-forming foam release sites other than fire-training areas: Field-validation of critical fate and transport properties, *Chemosphere*, 2016, **150**, 678–685.

14 G. Pitter, F. Da Re, C. Canova, G. Barbieri, M. Zare Jeddi, F. Daprà, F. Manea, R. Zolin, M. Bettega Anna, G. Stopazzolo, S. Vittorii, L. Zambelli, M. Martuzzi, D. Mantoan and F. Russo, Serum Levels of Perfluoroalkyl Substances (PFAS) in Adolescents and Young Adults Exposed to Contaminated Drinking Water in the Veneto Region, Italy: A Cross-Sectional Study Based on a Health Surveillance Program, *Environ. Health Perspect.*, 2020, **128**, 027007.

15 G. B. Post, Recent U.S. State and Federal Drinking Water Guidelines for Per- and Polyfluoroalkyl Substances, *Environ. Toxicol. Chem.*, 2021, **40**, 550–563.

16 S. M. Goodrow, B. Ruppel, R. L. Lippincott, G. B. Post and N. A. Procopio, Investigation of levels of perfluoroalkyl substances in surface water, sediment and fish tissue in New Jersey, USA, *Sci. Total Environ.*, 2020, **729**, 138839.

17 X. Bai and Y. Son, Perfluoroalkyl substances (PFAS) in surface water and sediments from two urban watersheds in Nevada, USA, *Sci. Total Environ.*, 2021, **751**, 141622.

18 T. Schwichtenberg, D. Bogdan, C. C. Carignan, P. Reardon, J. Rewerts, T. Wanzek and J. A. Field, PFAS and Dissolved Organic Carbon Enrichment in Surface Water Foams on a Northern U.S. Freshwater Lake, *Environ. Sci. Technol.*, 2020, **54**, 14455–14464.

19 E. Hepburn, C. Madden, D. Szabo, T. L. Coggan, B. Clarke and M. Currell, Contamination of groundwater with per- and polyfluoroalkyl substances (PFAS) from legacy landfills in an urban re-development precinct, *Environ. Pollut.*, 2019, **248**, 101–113.

20 L. W. Y. Yeung and S. A. Mabury, Are humans exposed to increasing amounts of unidentified organofluorine?, *Environ. Chem.*, 2016, **13**, 102–110.

21 A. Glynn, U. Berger, A. Bignert, S. Ullah, M. Aune, S. Lignell and P. O. Darnerud, Perfluorinated Alkyl Acids in Blood Serum from Primiparous Women in Sweden: Serial Sampling during Pregnancy and Nursing, And Temporal Trends 1996–2010, *Environ. Sci. Technol.*, 2012, **46**, 9071–9079.

22 K. A. Pike, P. L. Edmiston, J. J. Morrison and J. A. Faust, Correlation Analysis of Perfluoroalkyl Substances in Regional U.S. Precipitation Events, *Water Res.*, 2021, **190**, 116685.

23 O. Quiñones and S. A. Snyder, Occurrence of Perfluoroalkyl Carboxylates and Sulfonates in Drinking Water Utilities and Related Waters from the United States, *Environ. Sci. Technol.*, 2009, **43**, 9089–9095.

24 M. Sun, E. Arevalo, M. Strynar, A. Lindstrom, M. Richardson, B. Kearns, A. Pickett, C. Smith and D. R. U. Knappe, Legacy and Emerging Perfluoroalkyl Substances Are Important Drinking Water Contaminants in the Cape Fear River Watershed of North Carolina, *Environ. Sci. Technol. Lett.*, 2016, **3**, 415–419.

25 M. Ateia, A. Maroli, N. Tharayil and T. Karanfil, The overlooked short- and ultrashort-chain poly- and perfluorinated substances: A review, *Chemosphere*, 2019, **220**, 866–882.

26 S. Brendel, É. Fetter, C. Staude, L. Vierke and A. Biegel-Engler, Short-chain perfluoroalkyl acids: environmental concerns and a regulatory strategy under REACH, *Environ. Sci. Eur.*, 2018, **30**, 9.

27 J. Kjølholt, A. A. Jensen and M. Warming, *Short-chain Polyfluoroalkyl Substances (PFAS). A literature review of information on human health effects and environmental fate and effect aspects of short-chain PFAS*, Danish Ministry of Environment, 2015, Environmental Protection Agency report No 1707.

28 Z. Zhou, Y. Liang, Y. Shi, L. Xu and Y. Cai, Occurrence and Transport of Perfluoroalkyl Acids (PFAAs), Including Short-Chain PFAAs in Tangxun Lake, China, *Environ. Sci. Technol.*, 2013, **47**, 9249–9257.

29 S. A. Gannon, W. J. Fasano, M. P. Mawn, D. L. Nabb, R. C. Buck, L. W. Buxton, G. W. Jepson and S. R. Frame, Absorption, distribution, metabolism, excretion, and kinetics of 2,3,3,3-tetrafluoro-2-(heptafluoropropoxy)propanoic acid ammonium salt following a single dose in rat, mouse, and cynomolgus monkey, *Toxicology*, 2016, **340**, 1–9.

30 F. Li, J. Duan, S. Tian, H. Ji, Y. Zhu, Z. Wei and D. Zhao, Short-chain per- and polyfluoroalkyl substances in aquatic systems: Occurrence, impacts and treatment, *Chem. Eng. J.*, 2020, **380**, 122506.

31 J. L. Harfmann, K. Tito, R. J. Kieber, G. B. Avery, R. N. Mead, M. S. Shimizu and S. A. Skrabal, Sorption of Hexafluoropropylene Oxide Dimer Acid to Sediments: Biogeochemical Implications and Analytical Considerations, *ACS Earth Space Chem.*, 2021, **5**, 580–587.

32 W. Wang, A. Maimaiti, H. Shi, R. Wu, R. Wang, Z. Li, D. Qi, G. Yu and S. Deng, Adsorption behavior and mechanism of emerging perfluoro-2-propoxypropanoic acid (GenX) on activated carbons and resins, *Chem. Eng. J.*, 2019, **364**, 132–138.

33 D. Guo, Q. Shi, B. He and X. Yuan, Different solvents for the regeneration of the exhausted activated carbon used in the treatment of coking wastewater, *J. Hazard. Mater.*, 2011, **186**, 1788–1793.

34 K. Kim, S. Cotty, J. Elbert, R. Chen, C. H. Hou and X. Su, Asymmetric Redox-Polymer Interfaces for Electrochemical Reactive Separations: Synergistic Capture and Conversion of Arsenic, *Adv. Mater.*, 2020, **32**, e1906877.

35 Y. Kim, K. Kim, H. H. Eom, X. Su and J. W. Lee, Electrochemically-assisted removal of cadmium ions by redox active Cu-based metal-organic framework, *Chem. Eng. J.*, 2021, **421**, 129765.

36 K. Kim, P. Baldaguez Medina, J. Elbert, E. Kayiwa, R. D. Cusick, Y. Men and X. Su, Molecular Tuning of Redox-Copolymers for Selective Electrochemical Remediation, *Adv. Funct. Mater.*, 2020, 2004635.

37 L. Bromberg, N. Ozbek, K.-J. Tan, X. Su, L. P. Padhye and T. Alan Hatton, Iron phosphomolybdate complexes in electrocatalytic reduction of aqueous disinfection by-products, *Chem. Eng. J.*, 2021, **408**, 127354.

38 X. Su, L. Bromberg, K.-J. Tan, T. F. Jamison, L. P. Padhye and T. A. Hatton, Electrochemically Mediated Reduction of Nitrosamines by Hemin-Functionalized Redox Electrodes, *Environ. Sci. Technol. Lett.*, 2017, **4**, 161–167.

39 M. Ateia, A. Alsbaiee, T. Karanfil and W. Dichtel, Efficient PFAS Removal by Amine-Functionalized Sorbents: Critical Review of the Current Literature, *Environ. Sci. Technol. Lett.*, 2019, **6**, 688–695.

40 W. Ji, L. Xiao, Y. Ling, C. Ching, M. Matsumoto, R. P. Bisbey, D. E. Helbling and W. R. Dichtel, Removal of GenX and Perfluorinated Alkyl Substances from Water by Amine-Functionalized Covalent Organic Frameworks, *J. Am. Chem. Soc.*, 2018, **140**, 12677–12681.

41 I. Y. Zhukova, E. N. Papina and I. N. Tyaglivaya, Prospects of Wasteless Technologies of Selective Alcohols Oxidation, *IOP Conf. Ser.: Earth Environ. Sci.*, 2020, **459**, 032011.

42 U. S. G. Survey, Saline Water and Salinity, https://www.usgs.gov/special-topic/water-science-school/science/saline-water-and-salinity?qt-science_center_objects=0#qt-science_center_objects.

43 K. Hoffman, F. Webster Thomas, M. Bartell Scott, G. Weisskopf Marc, T. Fletcher and M. Vieira Verónica, Private Drinking Water Wells as a Source of Exposure to Perfluorooctanoic Acid (PFOA) in Communities Surrounding a Fluoropolymer Production Facility, *Environ. Health Perspect.*, 2011, **119**, 92–97.

44 J. Horst, J. McDonough, I. Ross and E. Houtz, Understanding and Managing the Potential By-Products of PFAS Destruction, *Groundwater Monit. Rem.*, 2020, **40**, 17–27.

45 M. Pierpaoli, M. Szopińska, B. K. Wilk, M. Sobaszek, A. Łuczkiewicz, R. Bogdanowicz and S. Fudala-Książek, Electrochemical oxidation of PFOA and PFOS in landfill leachates at low and highly boron-doped diamond electrodes, *J. Hazard. Mater.*, 2021, **403**, 123606.

46 Á. Soriano, D. Gorri, L. T. Biegler and A. Urtiaga, An optimization model for the treatment of perfluorocarboxylic acids considering membrane preconcentration and BDD electrooxidation, *Water Res.*, 2019, **164**, 114954.

47 H. Lin, J. Niu, J. Xu, H. Huang, D. Li, Z. Yue and C. Feng, Highly Efficient and Mild Electrochemical Mineralization of Long-Chain Perfluorocarboxylic Acids (C9–C10) by Ti/SnO2–Sb–Ce, Ti/SnO2–Sb/Ce–PbO2, and Ti/BDD Electrodes, *Environ. Sci. Technol.*, 2013, **47**, 13039–13046.

48 M. Panizza, in *Electrochemistry for the Environment*, ed. C. Comninellis and G. Chen, Springer New York, New York, NY, 2010, pp. 25–54, DOI: 10.1007/978-0-387-68318-8_2.

